

## Supporting information for: An alternative method to determine the bulk backbiting rate coefficient in acrylate radical polymerization

Yoshi W. Marien,<sup>1</sup> Paul H. M. Van Steenberge,<sup>1</sup> Katrin B. Kockler,<sup>2,3</sup> Christopher Barner-Kowollik,<sup>2,3,4\*</sup> Marie-Françoise Reyniers,<sup>1</sup> Dagmar R. D'hooge,<sup>1,5\*</sup> Guy B. Marin<sup>1</sup>

<sup>1</sup>Laboratory for Chemical Technology, Ghent University, Technologiepark 914, B-9052 Zwijnaarde (Ghent), Belgium.

<sup>2</sup>Preparative Macromolecular Chemistry, Institut für Technische Chemie und Polymerchemie, Karlsruhe Institute of Technology (KIT), Engesserstrasse 18, 76128 Karlsruhe, Germany

<sup>3</sup>Institut für Biologische Grenzflächen, Karlsruhe Institute of Technology (KIT), Hermann-von-Helmholtz-Platz 1, 76344 Eggenstein-Leopoldshafen, Germany

<sup>4</sup>School of Chemistry, Physics and Mechanical Engineering, Queensland University of Technology (QUT), 2 George Street, Brisbane, QLD 4000, Australia

<sup>5</sup>Department of Textiles, Ghent University, Technologiepark 907, B-9052 Zwijnaarde (Ghent), Belgium.

Corresponding authors: [dagmar.dhooge@ugent.be](mailto:dagmar.dhooge@ugent.be) [christopher.barner-kowollik@kit.edu](mailto:christopher.barner-kowollik@kit.edu) [christopher.barnerkowollik@qut.edu.au](mailto:christopher.barnerkowollik@qut.edu.au)

### Contents

1	Experimental details for the measurement of the inflection points.....	2
2	Model details for the calculation of the inflection points.....	3
2.1	Reactions and model parameters for the basic PLP model .....	3
2.2	Correction for SEC broadening .....	6
3	Robustness of the alternative method.....	8
3.1	Sensitivity of $k_{p,app}$ to the model parameters.....	8
3.1.1	Photodissociation .....	8
3.1.2	Chain transfer to monomer.....	9
3.1.3	Chain transfer to solvent .....	10
3.1.4	Termination .....	11
3.2	Simultaneous estimation of $k_{bb}$ and $k_{p,m}$ .....	12
4	References .....	14

## 1 Experimental details for the measurement of the inflection points

In this section, an overview of the experimental results is given. In Table S1, all the initial conditions and the corresponding results for the inflection points are listed. Typical PLP-SEC traces are shown in Figure S1 with an indication of the inflection points (black circles).

**Table S1.** Experimental results for PLP of *n*BuA at 303 K for varying solvent volume fraction and laser pulse frequency; initial conditions:  $[DMPA]_0 = 2.5 \cdot 10^{-3} \text{ mol L}^{-1}$ ,  $E_{\text{pulse}} = 1.5 \cdot 10^{-3} \text{ J}$ ; solvent: butyl propionate

Entry	Volume fraction solvent [-]	Frequency [ $\text{s}^{-1}$ ]	Number of pulses [-]	$k_{p,\text{app}}$ [ $\text{L mol}^{-1} \text{ s}^{-1}$ ]
1	0	10	25	4366
2	0	20	35	7820
3	0	40	45	8913
4	0	60	55	9873
5	0.5	10	35	3727
6	0.5	20	45	4575
7	0.5	40	65	6218
8	0.5	60	75	7816
9	0.75	10	50	2858
10	0.75	20	65	4193
11	0.75	40	85	5179
12	0.75	60	95	7152

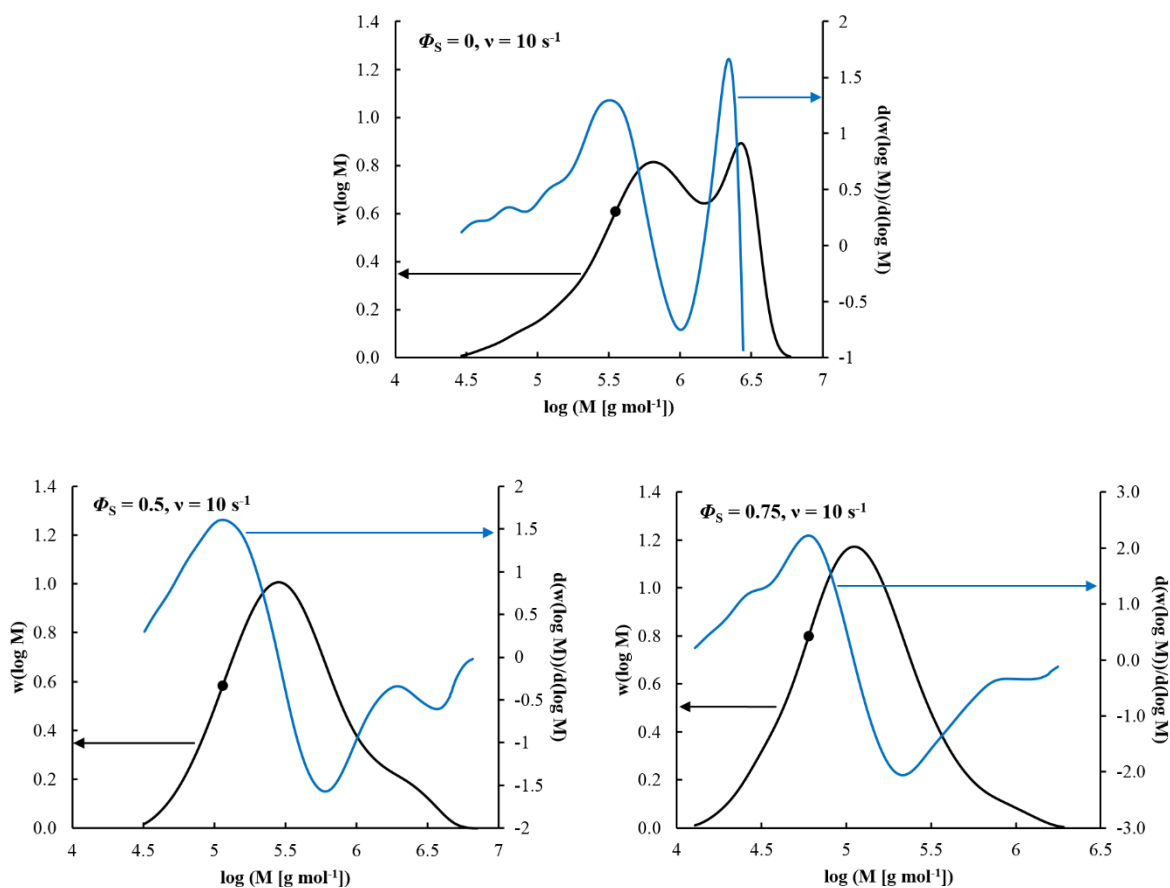


**Figure S1.** Typical measured PLP-SEC traces (full black line) and their corresponding first derivative (full blue line) for PLP of *n*BuA at 303 K for varying solvent volume fraction ( $\Phi_S = 0, 0.5, 0.75$ ) and a laser pulse frequency  $\nu = 10 \text{ s}^{-1}$ ; black circle: inflection point (*i.e.* maximum of first derivative) used for  $k_{p,app}$  determination (Equation (2) in the main text); initial conditions:  $[\text{DMPA}]_0 = 2.5 \cdot 10^{-3} \text{ mol L}^{-1}$ ,  $E_{\text{pulse}} = 1.5 \cdot 10^{-3} \text{ J}$ ; solvent: butyl propionate (see also Table S1).

## 2 Model details for the calculation of the inflection points

### 2.1 Reactions and model parameters for the basic PLP model

An overview of the reactions considered in the kinetic Monte Carlo (*k*MC) model to calculate the inflection points and thus to obtain the simulated input for the regression analysis is provided in Table S2 (basic reaction scheme). In the same table, the model parameters for the theoretical evaluation of the method (parameters: only typical orders of magnitude) and the application to the actual experimental data (*cf.* Table S1) are included.

**Table S2.** Basic reaction scheme to simulate low temperature PLP of *n*BuA initiated by DMPA, including a listing of the model parameters used for the theoretical evaluation of the method (only orders of magnitude) and the actual application to *n*BuA at 303 K; intermolecular chain transfer,  $\beta$ C-scission and macromonomer addition neglected based on literature data.<sup>1, 2</sup> Chain transfer to monomer and solvent can be also neglected, as demonstrated in Section 3.

Reaction	Equation	Theoretical evaluation $\Delta[R_0]$ [mol L <sup>-1</sup> ], $k$ [(L mol <sup>-1</sup> ) s <sup>-1</sup> ]	<i>n</i> BuA 303 K $\Delta[R_0]$ [mol L <sup>-1</sup> ], $k$ [(L mol <sup>-1</sup> ) s <sup>-1</sup> ]
Photodissociation <sup>[a]</sup>	$DMPA \xrightarrow{\Delta[R_0]} R_{0,e}^I + R_{0,e}^{II}$	10 <sup>-4</sup>	2 10 <sup>-5</sup>
Chain initiation <sup>[b]</sup>	$R_{0,e}^{I/III} + M \xrightarrow{k_{p,I/III}} R_{1,e}$	10 <sup>4</sup>	1.8 10 <sup>4</sup>
Propagation	$R_{i,e} + M \xrightarrow{k_{p,e}} R_{i+1,e}$	10 <sup>4</sup>	1.8 10 <sup>4</sup> [3]
	$R_{i,m} + M \xrightarrow{k_{p,m}} R_{i+1,e}$	10 <sup>2</sup>	1.2 10 <sup>1</sup> [4]
Backbiting ( $i \geq 3$ )	$R_{i,e} \xrightarrow{k_{bb}} R_{i,m}$	10 <sup>3</sup>	1.7 10 <sup>2</sup>
Termination <sup>[c]</sup> ( $i, j \geq 0$ )	$R_{i,e} + R_{j,e} \xrightarrow{k_{t,ee}^{app}(i,j)} P_{i(+j)}(+P_j)$	10 <sup>9</sup>	9.3 10 <sup>8</sup> [4]
	$R_{i,e} + R_{j,m} \xrightarrow{k_{t,em}^{app}(i,j)} P_{i(+j)}(+P_j)$	10 <sup>8</sup>	6.1 10 <sup>8</sup> [4]
	$R_{i,m} + R_{j,m} \xrightarrow{k_{t,mm}^{app}(i,j)} P_{i(+j)}(+P_j)$	10 <sup>6</sup>	1.9 10 <sup>6</sup> [4]

<sup>a</sup>: dissociation into a benzoyl and dimethoxy benzyl radical;  $\Delta[R_0]$  of the first laser pulse is reported (Equation (S.3))

<sup>b</sup>:  $k_{p,I/III}$  can be taken equal to the plateau value for propagation with long ECRs, no propagation of  $R_{0,II}$  (*see* Subsection 2.1)

<sup>c</sup>: chain length dependent (apparent) termination rate coefficients according to the composite  $k_t$  model are considered (*see* Subsection 2.1);  $k_t^{app}(1,1)$  is reported, taking into account a correction with a factor 2, as indicated by *e.g.* Derboven *et al.*;<sup>5</sup> fraction termination by recombination ( $\delta$ ) in agreement with literature data ( $\delta_{ee} = 0.9$ ,  $\delta_{em} = 0.3$ ,  $\delta_{mm} = 0.1$ )<sup>2, 6</sup>;  $i, j = 0$ :  $R_{0,e}^{I/III/III}$

In what follows, specific attention is focused on the kinetic parameters for photodissociation, chain initiation, and termination. In Section 3 it is demonstrated that the reactions included are indeed sufficient for the reliable calculation of the inflection points.

The generated amount of photoinitiator radical fragments per pulse ( $\Delta[R_0]$ ) is calculated explicitly.<sup>7</sup> The rate of photodissociation (mol L<sup>-1</sup> s<sup>-1</sup>) as a function of the intensity delivered by the light source ( $I_0$ ; W dm<sup>-2</sup>) is calculated as:

$$r_{diss} = \Phi_{diss} \frac{I_0 \lambda}{hc N_A L} [1 - \exp(-2.303 \varepsilon [DMPA] L)] \quad (S.1)$$

with  $\Phi_{\text{diss}}$  the quantum yield for photodissociation (0.95;<sup>8</sup> also see subsection 3.1.1),  $\lambda$  the wavelength of the laser (351  $10^{-7}$  cm),  $\varepsilon$  the molar absorptivity of the photoinitiator (280 L mol<sup>-1</sup> cm<sup>-1</sup>),  $L$  the optical path length (0.78 cm),  $h$  the Planck constant (6.63  $10^{-34}$  J s),  $c$  the speed of light (3  $10^9$  dm s<sup>-1</sup>), and  $N_A$  the Avogadro constant (6.02  $10^{23}$  mol<sup>-1</sup>). The intensity ( $I_0$ ) can be expressed as a function of the laser pulse energy ( $E_{\text{pulse}}$ ; 1.5  $10^{-3}$  J):

$$I_0 = \frac{E_{\text{pulse}}}{\Omega \Delta t_{\text{pulse}}} \quad (\text{S.2})$$

with  $\Omega$  the optical cross-sectional area (3.85  $10^{-3}$  dm<sup>2</sup>) and  $\Delta t_{\text{pulse}}$  the duration of the pulse. Since the change in DMPA concentration during a pulse can be assumed to be negligible (initial [DMPA] = 2.5  $10^{-3}$  mol L<sup>-1</sup>),  $\Delta[R_0]$  can be calculated by multiplying  $r_{\text{diss}}$  (Equation (S.1)) with  $\Delta t_{\text{pulse}}$ , taking into account a factor 2 (two radicals formed per dissociation reaction):

$$\Delta[R_0] = 2\Phi_{\text{diss}} \frac{E_{\text{pulse}} \lambda}{hc N_A \Omega L} [1 - \exp(-2.303 \varepsilon [\text{DMPA}] L)] \quad (\text{S.3})$$

In agreement with earlier kinetic analysis of single pulse-pulsed laser polymerization (SP-PLP) experiments,<sup>9</sup> and based on literature data,<sup>10-13</sup> in the present work, the difference in chain initiation reactivity of the DMPA radical initiator fragments (entry 2 in Table S2) is taken into account. No further decomposition needs to be taken into account due to the selected low polymerization temperature of 303 K.<sup>9</sup>

Chain length dependent termination kinetics - either caused intrinsically or by diffusional limitations - are evaluated via the composite  $k_t$  model.<sup>14-17</sup> For the low monomer conversion ranges as encountered during PLP, it suffices to consider:

$$k_t^{app}(i, i) = k_t^{app}(1, 1) i^{-\alpha_S} \quad i \leq i_c \quad (\text{S.4})$$

$$k_t^{app}(i, i) = k_t^{app}(1, 1) i_c^{-\alpha_S + \alpha_L} i^{-\alpha_L} \quad i > i_c \quad (\text{S.5})$$

in which  $\alpha_S$  and  $\alpha_L$  express the chain length dependence for short and long radicals, and  $i_c$  is the cross-over chain length. The values as reported by Barth *et al.*<sup>4</sup> are used, *i.e.*  $\alpha_S = 0.85$ ,  $\alpha_L = 0.16$ , and  $i_c = 30$ .

## 2.2 Correction for SEC broadening

When designing and interpreting PLP-SEC experiments, it has to be taken into account that axial dispersion during analysis leads to a broadening. Buback *et al.*<sup>18</sup> have proposed a procedure to account for this experimental broadening, based on principles suggested by Tung<sup>19</sup> and Billiani.<sup>20</sup>

Tung<sup>19</sup> proposed to express the chromatogram  $f$  as the convolution of the chromatogram in case no experimental broadening would occur,  $h$ , with a broadening function  $G$ :

$$f(v) = \int_0^{+\infty} G(v - \tilde{v}) h(\tilde{v}) d\tilde{v} \quad (\text{S.6})$$

According to Billiani<sup>20</sup> the broadening function can be represented by a Gaussian distribution with variance  $\sigma_v^2$ :

$$G(v - \tilde{v}) = \frac{1}{\sigma_v \sqrt{2\pi}} \exp\left(-\frac{(v - \tilde{v})^2}{2\sigma_v^2}\right) \quad (\text{S.7})$$

Shortt<sup>21</sup> demonstrated that the relation between the broadened MMD  $w_{SEC}(\log M)$  and the chromatogram  $f(v)$  is given by:

$$w_{SEC}(\log M) = -\frac{f(v)}{d(\log M)/dv} \quad (\text{S.8})$$

Analogously, the relation between  $w(\log M)$ , with  $M$  representing the molar mass, and the chromatogram  $h(v)$ , with  $w(\log M)$  and  $h(v)$  both representing the case no broadening occurs, is given by:

$$w(\log M) = -\frac{h(v)}{d(\log M)/dv} \quad (\text{S.9})$$

If the relation between the elution volume  $v$  and  $\log M$  is linear:

$$\log M = a - bv \quad (\text{S.10})$$

it follows that:

$$\frac{d(\log M)}{dv} = -b \quad (\text{S.11})$$

Substituting (S.11) into (S.8) and (S.9), respectively, yields:

$$f(v) = b w_{SEC}(\log M) \quad (\text{S.12})$$

$$h(v) = b w(\log M) \quad (\text{S.13})$$

Finally, substituting (S.7), (S.12), and (S.13) into (S.6), yields:

$$w_{SEC}(\log M) = \frac{1}{(2\pi)^{0.5} \sigma_v b} \int_0^{+\infty} \exp\left(-\frac{(\log(M) - \log(\tilde{M}))^2}{2(\sigma_v b)^2}\right) w(\log \tilde{M}) d\log(\tilde{M}) \quad (\text{S.14})$$

Equation (S.14) has the important implication that broadening is assumed Gaussian with respect to  $\log(M)$  and, hence, larger chain lengths will SEC-broaden exponentially. The SEC broadening parameter  $(\sigma_v b)$  can be determined via regression to the SEC-measured MMD for a narrow polystyrene standard. It can be expected that this leads to an upper limit for the broadening parameter, as this value also reflects the width of the MMD of the polystyrene standard. It has been opted in the present work to use the literature value of  $4 \cdot 10^{-2}$ .<sup>22</sup>

### 3 Robustness of the alternative method

In the present section, the robustness of the alternative method is illustrated. Via a sensitivity analysis it is first demonstrated that a correct calculation of inflection points does not imply the need of a detailed model with highly accurate kinetic parameters. Next it is shown that the method can in principle be applied for the simultaneous estimation of the backbiting and mid-chain radical propagation rate coefficient, indicating that a lack of knowledge on the latter does not lead to a failure of the method.

#### 3.1 Sensitivity of $k_{p,app}$ to the model parameters

##### 3.1.1 Photodissociation

In this work,  $\Delta[R_0]$  is fundamentally calculated via Equation (S.3) by substituting the values for the experimental parameters ( $E_{\text{pulse}} = 1.5 \cdot 10^{-3}$  J,  $[\text{DMPA}] = 2.5 \cdot 10^{-3}$  mol L<sup>-1</sup>,  $\lambda = 351 \cdot 10^{-7}$  cm,  $\Omega = 3.85 \cdot 10^{-3}$  dm<sup>2</sup>,  $L = 0.78$  cm), the physical constants ( $h = 6.63 \cdot 10^{-34}$  J s,  $c = 3 \cdot 10^9$  dm s<sup>-1</sup>,  $N_A = 6.02 \cdot 10^{23}$  mol<sup>-1</sup>) and physicochemical coefficients ( $\epsilon = 280$  L mol<sup>-1</sup> cm<sup>-1</sup> and  $\Phi_{\text{diss}} = 0.95$ ). It should be noted that  $\Phi_{\text{diss}}$  has been also reported equal to 0.52;<sup>23</sup> in contrast to the value reported by Allonas *et al.*<sup>8</sup> ( $\Phi_{\text{diss}} = 0.95$ ). For  $\Phi_s = 0$  and  $\nu = 10$  s<sup>-1</sup> the effect of such a variation in  $\Phi_{\text{diss}}$  (and thus  $\Delta[R_0]$ ) on the PLP-SEC trace and in particular on the position of the inflection point is shown to be negligible in Figure S2 (full purple line:  $\Phi_{\text{diss}} = 0.95$ ,  $L_1 = 3778$ ; dashed yellow line:  $\Phi_{\text{diss}} = 0.52$ ,  $L_1 = 3851$ ).



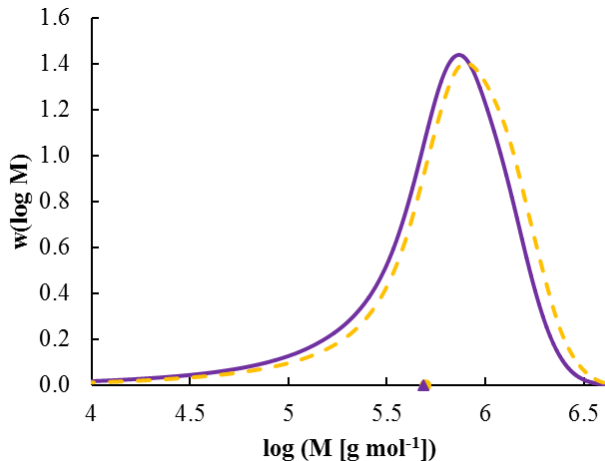


**Figure S2.** Theoretical illustration of the negligible effect of a possible variation of  $\Phi_{\text{diss}}$  on the PLP-SEC trace (full purple line:  $\Phi_{\text{diss}} = 0.95$ ; dashed yellow line:  $\Phi_{\text{diss}} = 0.52$ ) and in particular on the inflection point (symbols) for  $\Phi_S = 0$  and  $\nu = 10 \text{ s}^{-1}$ ; initial conditions: Table S1; model parameters: Table S2.

### 3.1.2 Chain transfer to monomer

In principle the estimated parameter values could depend on the chain transfer to monomer rate coefficients  $k_{\text{trM,e}}$  (transfer from an ECR) and  $k_{\text{trM,m}}$  (transfer from an MCR). In Figure S3 it is theoretically demonstrated that at the temperature considered in this study (303 K), chain transfer to monomer has a negligible effect on the PLP-SEC trace (dashed yellow line:  $k_{\text{trM,e}} = 6.9 \cdot 10^{-1} \text{ L mol}^{-1} \text{ s}^{-1}$  and  $k_{\text{trM,m}} = 2.3 \cdot 10^{-3} \text{ L mol}^{-1} \text{ s}^{-1}$  (literature values<sup>24</sup>),  $L_1 = 3528$ ; full purple line:  $k_{\text{trM,e}} = k_{\text{trM,m}} = 0 \text{ L mol}^{-1} \text{ s}^{-1}$ ,  $L_1 = 3778$ ) and in particular on the position of the inflection point (symbols in Figure S3), even under the conditions of the highest importance of chain transfer to monomer, *i.e.* highest monomer concentration ( $\Phi_S = 0$ ) and lowest frequency ( $\nu = 10 \text{ s}^{-1}$ ) considered in this study.

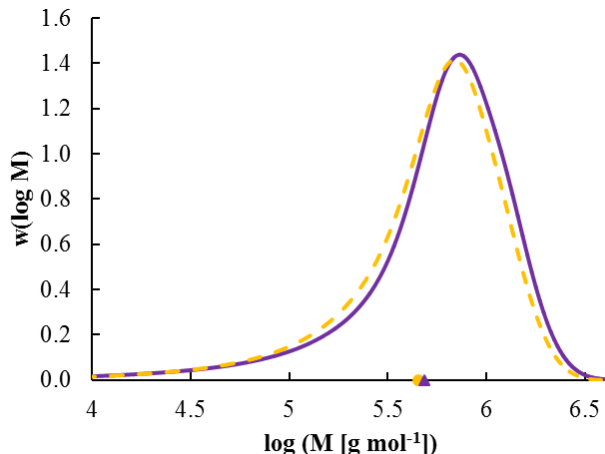


**Figure S3.** Theoretical illustration of the negligible effect of chain transfer to monomer on the PLP-SEC trace and in particular on the inflection point at 303 K; transfer to monomer accounted for (dashed yellow line;  $k_{\text{trM,e}}$  and  $k_{\text{trM,m}}$  from ref.<sup>24</sup>) and neglected (full purple line;  $k_{\text{trM,e}} = k_{\text{trM,m}} = 0 \text{ L mol}^{-1} \text{ s}^{-1}$ );  $\Phi_S = 0$ ,  $v = 10 \text{ s}^{-1}$  (*i.e.* conditions corresponding to the highest importance of chain transfer to monomer); initial conditions: Table S1; model parameters: Table S2.

### 3.1.3 Chain transfer to solvent

In addition to chain transfer to monomer, chain transfer to solvent can occur. In order to investigate the effect of this chain transfer reaction on the PLP-SEC trace and in particular on the inflection point, simulations with the coefficient of chain transfer to solvent ( $C_{\text{trS}}$ ) based on literature data are performed.  $C_{\text{trS}}$  is assessed by the value for chain transfer from poly(ethyl acrylate) radicals to ethyl acetate at 353 K ( $C_{\text{trS}} = 8.9 \cdot 10^{-5}$ ).<sup>25</sup> The value of  $C_{\text{trS}}$  at 353 K is converted to the value at 303 K using for simplicity the activation energy of the rate coefficient of chain transfer to monomer ( $C_{\text{trM}}$ ), which yields a value for  $C_{\text{trS}}$  of  $3.9 \cdot 10^{-5}$ . In Figure S4, the PLP-SEC trace for  $C_{\text{trS}} = 3.9 \cdot 10^{-5}$  (dashed yellow line;  $L_1 = 465$ ) and  $C_{\text{trS}} = 0$  (full blue line;  $L_1 = 496$ ) is shown, with the inflection point indicated by a symbol. It is clear that at 303 K, chain transfer to solvent has a negligible effect on the PLP-SEC trace and thus on the inflection point, even under the conditions of the highest importance of chain transfer to solvent, *i.e.* highest

solvent volume fraction ( $\Phi_S = 0.75$ ) and lowest frequency ( $\nu = 10 \text{ s}^{-1}$ ) considered in this study. Hence, chain transfer to solvent can safely be neglected in the present work and no accurate rate coefficients need to be known for the reliable estimation of  $k_{bb}$  and  $k_{p,m}$ . In addition, in general, the temperature and frequencies can always be regulated to avoid a possible impact.

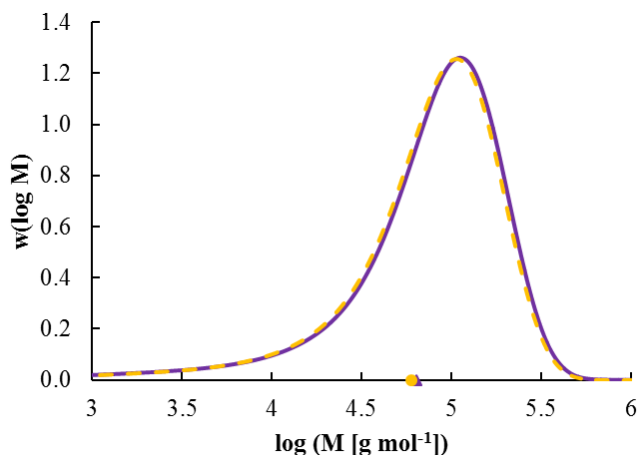


**Figure S4.** Theoretical illustration of the negligible effect of chain transfer to solvent on the PLP-SEC trace and in particular on the inflection point at 303 K; transfer to solvent accounted for (dashed yellow line;  $C_{\text{trS}}$  based on ref<sup>25</sup>) and neglected (full purple line;  $C_{\text{trS}} = 0 \text{ L mol}^{-1} \text{ s}^{-1}$ );  $\Phi_S = 0.75$ ,  $\nu = 10 \text{ s}^{-1}$  (*i.e.* conditions corresponding to the highest importance of chain transfer to solvent); initial conditions: Table S1; model parameters: Table S2.

### 3.1.4 Termination

Finally, the estimated parameter value for  $k_{bb}$  (and  $k_{p,m}$ ) could depend on the apparent termination reactivities. In Figure S5 it is demonstrated for  $\Phi_S = 0$  and  $\nu = 10 \text{ s}^{-1}$  that a significant variation of the termination reactivity (variation of  $k_t(1,1)$  by a factor 2) results in a shift of the PLP-SEC trace (full purple line: literature value for  $k_t(1,1)$ ,<sup>4</sup>  $L_1 = 3778$ ; dotted blue line:  $k_t(1,1) \times 2$ ,  $L_1 = 3638$ ; dashed yellow line:  $k_t(1,1) : 2$ ,  $L_1 = 3913$ ); the variation of the position of the inflection point is however negligible. Note that for a general monomer always a quick tuning of this parameter can be performed by considering the shift of the complete trace.

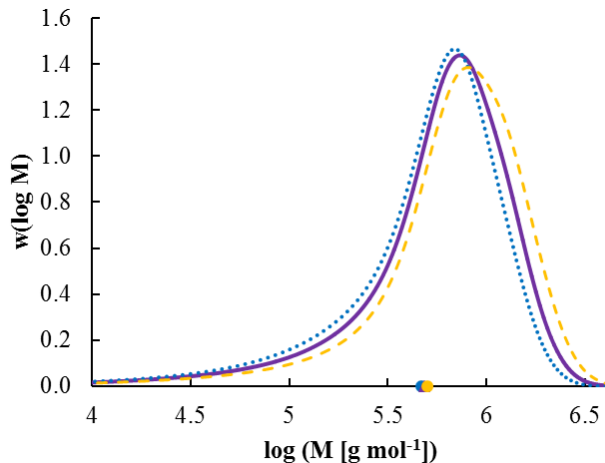


**Figure S5.** Theoretical illustration of the limited effect of the termination reactivity on the position of the inflection point (symbols) for  $\Phi_S = 0$  and  $v = 10 \text{ s}^{-1}$ ; full purple line: literature value for  $k_t(1,1)$ ,<sup>4</sup> dotted blue line:  $k_t(1,1) \times 2$ , dashed yellow line:  $k_t(1,1) : 2$ ; initial conditions: Table S1; model parameters: Table S2.

### 3.2 Simultaneous estimation of $k_{bb}$ and $k_{p,m}$

In the main text, the high accuracy of the method to estimate bulk  $k_{bb}$  values provided that  $k_{p,m}$  is accurately known is demonstrated (Figure 1). In this section, it is theoretically illustrated that in addition to  $k_{bb}$ ,  $k_{p,m}$  can also be accurately estimated provided that sufficient PLP-SEC inflection point data are available.

In agreement with the main text (Figure 1 (left)), regression analysis of *in silico*  $k_{p,app}$  data perturbed by a Gaussian error with a standard deviation of  $400 \text{ L mol}^{-1} \text{ s}^{-1}$  (*i.e.* a relative error of ca. 10%) is performed, however this time aiming at the estimation of both  $k_{bb}$  and  $k_{p,m}$ . For all rate coefficients typical orders of magnitude are again used (Table S2). A  $k_{bb}$  and  $k_{p,m}$  value of  $1012 \text{ s}^{-1}$  and  $102 \text{ L mol}^{-1} \text{ s}^{-1}$  are obtained with the corresponding fits shown in Figure S6 (full lines). The obtained estimates ( $1012 \pm 307 \text{ s}^{-1}$  and  $102 \pm 40 \text{ L mol}^{-1} \text{ s}^{-1}$ ) are thus very close to the implemented and to be estimated value of  $1000 \text{ s}^{-1}$  and  $100 \text{ L mol}^{-1} \text{ s}^{-1}$  (Table S2); statistical analysis indicates a correlation coefficient of 0.83, which is sufficiently low highlighting the

limited correlation between the parameters. Large individual 95% confidence intervals are however obtained as only a small data set is considered. Hence, in case both parameters need to be estimated for an actual experimental data set it can be concluded that this set needs to be larger, in particular in case of high experimental errors.

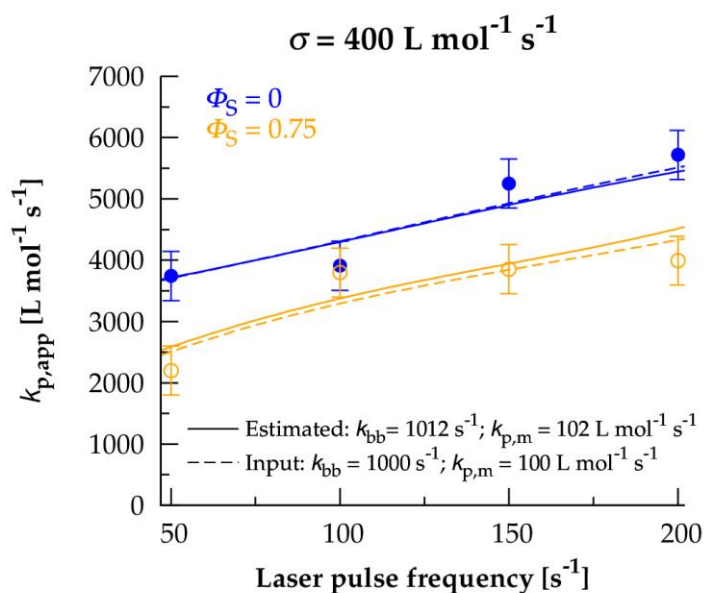


**Figure S6.** Potential of the method to estimate both  $k_{bb}$  and  $k_{p,m}$  for acrylate radical polymerization from  $k_{p,app}$  data (Equation 2); symbols: generated data with the  $kMC$  model (dashed lines), superimposed with an artificial error with a standard deviation  $\sigma$  (same as in Figure 1 (left) in the main text; model parameters: Table S2; full lines: fits after regression analysis.

## 4 References

1. J. Barth, M. Buback, P. Hesse and T. Sergeeva, *Macromol. Rapid Commun.*, 2009, **30**, 1969-1974.
2. A. N. Nikitin, R. A. Hutchinson, W. Wang, G. A. Kalfas, J. R. Richards and C. Bruni, *Macromol. React. Eng.*, 2010, **4**, 691-706.
3. J. M. Asua, S. Beuermann, M. Buback, P. Castignolles, B. Charleux, R. G. Gilbert, R. A. Hutchinson, J. R. Leiza, A. N. Nikitin, J. P. Vairon and A. M. van Herk, *Macromol. Chem. Phys.*, 2004, **205**, 2151-2160.
4. J. Barth, M. Buback, P. Hesse and T. Sergeeva, *Macromolecules*, 2010, **43**, 4023-4031.
5. P. Derboven, D. R. D'hooge, M.-F. Reyniers, G. B. Marin and C. Barner-Kowollik, *Macromolecules*, 2015, **48**, 492-501.
6. S. Hamzehlou, N. Ballard, Y. Reyes, A. Aguirre, J. M. Asua and J. R. Leiza, *Polym. Chem.*, 2016, **7**, 2069-2077.
7. G. Odian, *Principles of Polymerization*, Wiley, 2004.
8. X. Allonas, J. Lalevee and J. P. Fouassier, *Journal of Photochemistry and Photobiology a-Chemistry*, 2003, **159**, 127-133.
9. M. Buback, M. Busch and C. Kowollik, *Macromol. Theory Simul.*, 2000, **9**, 442-452.
10. H. Fischer, R. Baer, R. Hany, I. Verhoolen and M. Walbiner, *J. Chem. Soc.-Perkin Trans. 2*, 1990, 787-798.
11. C. Barner-Kowollik, P. Vana and T. P. Davis, *J. Polym. Sci. Pol. Chem.*, 2002, **40**, 675-681.
12. Z. Szablan, T. M. Lovestead, T. P. Davis, M. H. Stenzel and C. Barner-Kowollik, *Macromolecules*, 2007, **40**, 26-39.
13. Z. Szablan, T. Junkers, S. P. S. Koo, T. M. Lovestead, T. P. Davis, M. H. Stenzel and C. Barner-Kowollik, *Macromolecules*, 2007, **40**, 6820-6833.
14. G. B. Smith, G. T. Russell and J. P. A. Heuts, *Macromol. Theory Simul.*, 2003, **12**, 299-314.
15. G. Johnston-Hall and M. J. Monteiro, *J. Polym. Sci. Pol. Chem.*, 2008, **46**, 3155-3173.
16. C. Barner-Kowollik and G. T. Russell, *Prog. Polym. Sci.*, 2009, **34**, 1211-1259.
17. J. B. L. de Kock, B. Klumperman, A. M. van herk and A. L. German, *Macromolecules*, 1997, **30**, 6743-6753.
18. M. Buback, M. Busch and R. A. Lammel, *Macromol. Theory Simul.*, 1996, **5**, 845-861.
19. L. H. Tung and J. R. Runyon, *J. Appl. Polym. Sci.*, 1969, **13**, 2397-&.
20. J. Billiani, G. Rois and K. Lederer, *Chromatographia*, 1988, **26**, 372-376.
21. D. W. Shortt, *J Liq Chromatogr*, 1993, **16**, 3371-3391.
22. A. N. Nikitin, R. A. Hutchinson, M. Buback and P. Hesse, *Macromolecules*, 2007, **40**, 8631-8641.
23. U. Muller and C. Vallejos, *Angewandte Makromolekulare Chemie*, 1993, **206**, 171-191.
24. S. Maeder and R. G. Gilbert, *Macromolecules*, 1998, **31**, 4410-4418.
25. J. Brandrup, *Polymer Handbook (4th Edition)*, John Wiley & Sons, 2005.